

Modeling of Diffusion NMR Using Non-Linear Magnetic Gradients

M.Sc. Thesis, June 2013

Nathalie Carius

Supervisor
Matias Nordin

2nd Supervisor
Maja Sohlin

Department of Radiation Physics
University of Gothenburg
Gothenburg, Sweden



Abstract

In this thesis the possibility to get information about a material's structure by using NMR technique has been investigated. A computer simulation was made for diffusing particles in different environments in order to investigate diffusion dependence on the material structure. How the particles diffuse can be studied with NMR using Pulsed Gradient Spin Echo method. By comparing a detected signal for linear gradient fields of different slopes, any influence from the structure of the material was investigated. Also studied was the possibility that a sinus shaped gradient field gives a better understanding of the structure. The result indicates that in the linear case the distribution gives information about the material structure. For the sinus case results were not conclusive due to statistical effects. A weak dependence is indicated of the response on the match between the spatial wavelength of the gradient field and the size of the material structures. This study should be repeated with more optimal choice of parameter values.

Contents

| | | |
|----------|---|-----------|
| 1 | Introduction | 7 |
| 2 | Theory and Background | 9 |
| 2.1 | Background | 9 |
| 2.2 | Diffusion | 9 |
| 2.3 | Nuclear Magnetic Resonance | 10 |
| 2.3.1 | Particle Spin and Magnetization | 10 |
| 2.3.2 | The NMR Signal | 12 |
| 2.3.3 | Sinus Gradient Field | 14 |
| 3 | Method of Investigation | 17 |
| 3.1 | The Monte Carlo Code | 17 |
| 3.1.1 | Code Structure | 17 |
| 3.1.2 | Particle Sources | 18 |
| 3.1.3 | Particle Direction | 18 |
| 3.2 | The Different Investigations | 20 |
| 3.2.1 | Diffusion | 20 |
| 3.2.2 | Magnetization | 22 |
| 3.2.3 | NMR Signal | 22 |
| 3.2.4 | Material Structure | 23 |
| 3.2.5 | Sinusoidal Field | 23 |
| 4 | Results | 25 |
| 4.1 | Diffusion | 25 |
| 4.2 | NMR | 26 |
| 5 | Discussion and Conclusions | 39 |
| | Acknowledgement | 43 |
| | Bibliography | 45 |

Chapter 1

Introduction

By using the phenomenon of nuclear magnetic resonance (NMR), a signal can be detected from a material, which might carry information about the material and its structure. This is anticipated since the charged atomic nuclei have spin and thus also a magnetic dipole moment, which interacts with external magnetic fields.

In 1938 Isidor Rabi initiated development of NMR. Later in 1946 (Nobel prize 1952) Felix Bloch and Edward Mills Purcell [1] further developed the theory by extending it to liquids and solids. In 1952 Herman Carr and Purcell used a magnetic field gradient to produce the first magnetic resonance image (MRI) in one dimension [2]. Using the new technique they could accurately measure the self-diffusion coefficients for fluids. Today the use of the magnetic resonance technique both clinically and in research has become a standard tool.

By the use of the NMR techniques it is possible to observe diffusion of particles in a material. Since diffusion is strongly material dependent, it is interesting to find out if it can bring information about material structure as well. This is the starting point of the present project.

In this master thesis work a computer simulation code is developed based on Monte Carlo techniques. Diffusing particles carrying spin are simulated in one and two dimensions under several conditions. Two different types of static magnetic fields are studied, a linearly varying field with constant gradient and a field with sinusoidal variation. It is of special interest to understand if there is a particular choice of spatial wavelength for the magnetic field variation that maximizes sensitivity for certain size structures in the observed material.

Chapter 2

Theory and Background

The theory which the NMR technique builds upon includes quantum mechanics and modern signal analysis. Relevant for this work is particle spin behavior in response to a magnetic field and how the magnetization signal is influenced by diffusion and possible material structures. The study of this research area includes several previous projects. The theoretical basis described in this chapter is divided into three major subjects being diffusion, particle spin and magnetization, and the NMR signal.

2.1 Background

This project builds on the work done by Grebenkov [3], who made a theoretical calculation for particles diffusing in one dimension between two planes under the influence of a gradient magnetic field having a sinusoidal variation. It is also a continuation of the work done by Linse and Söderman [4]. They simulated molecular diffusion between planes. The present work is based on the theory by Price describing how pulsed-field gradient NMR can be a tool for understanding and studying diffusion. It is explained in reference [5].

2.2 Diffusion

Diffusion is the phenomenon when atoms in a material gradually move because of the spontaneous motion of all particles in a material (due to temperature), and will result in a so called random walk or Brownian motion [6]. The rate of diffusion changes with the type of diffusing particle and the material they are diffusing in. The rate of diffusion can be described by the diffusion constant D . In the case of free diffusion it can be described by the the standard deviation (σ) of a Gaussian distribution of diffusing particles.

According to Einstein's theory for diffusion [7] they have the follow relation

$$D = \frac{\sigma^2}{n} \quad (2.1)$$

where n is the number of dimensions.

The diffusion in this project will be free in two dimensions, i.e. $n = 2$. This means that the particles will randomly walk in every direction in the plane with equal probability, i.e. the medium is isotropic and D is a scalar. The particles that are simulated will be protons in a fictitious material depending on the diffusion constant. All units will be arbitrary units (a.u.) which corresponds to rescaling of diffusion parameters.

2.3 Nuclear Magnetic Resonance

The MRI techniques are based on fundamental physical principles. Subatomic particles carry the quantum mechanical property called spin being associated with a magnetic dipole moment. Collectively many particles thus can give rise to a measurable magnetization field in a material. Furthermore, quantum mechanical properties make energy transfer through resonance possible with an external radio frequent electromagnetic field. These basics are discussed in subsection 2.3.1 whereas 2.3.2 describes how a recordable signal is achieved. Subsection 2.3.3 introduces the case of a sinusoidal gradient field.

2.3.1 Particle Spin and Magnetization

Elementary particles constituting matter carry a property called spin. This includes protons which are most commonly used in Nuclear Magnetic Resonance Imaging. The charged particle's spin creates a magnetic dipole moment (μ) and if a strong external magnetic field (B) is applied, the particle spin will interact with the external field. According to quantum mechanics [8] the particles are forced to orient their spins relative to the field direction, the so called gyromagnetic effect. Protons have spin $1/2$ (units of \hbar) and therefore only two possible states. The spin projection onto the B field direction (usually taken as z direction) is forced to be $\pm 1/2$. The z component of their dipole moment μ_z is thus parallel or antiparallel to B . Each spin state corresponds to a potential energy due to the dipole moment interacting with the

external magnetic field B , which is described by classical electrodynamics. This results in an energy difference ΔE between the two states:

$$\Delta E = 2\mu_z B = \gamma \hbar B \quad (2.2)$$

where $\mu_z = \gamma m \hbar$ is the z-component of the proton dipole moment and $m = \pm 1/2$ is the quantum number for the spin projection onto the z-axis. γ is the gyromagnetic ratio, which for the proton is

$$\gamma_p = \frac{g_p e}{2m_p} = 2\pi \cdot 42.576 \text{ MHz/T} \quad (2.3)$$

where g_p is the g-factor for protons, e is the elementary charge and m_p is the proton mass.

The spin and dipole moment will have a specific angle relative to the B field lines and, consequently, precess around these. The majority of the protons will orient themselves so they precess in positive direction (lower energy state) around the external field. As there are two possible orientations for the spin some of the protons could precess in negative direction (higher energy state). The net magnetization M will, however, be in the direction of the external magnetic field, since the lower energy state will be more populated at thermal equilibrium due to Boltzmann statistics $e^{-\Delta E/kT}$. The fact that the proton spin has a specific angle to the B field implies it has a dipole component μ_{\perp} perpendicular to B , which precesses around the field lines. The classical precession frequency f is called the Larmor frequency and corresponds to the photon energy $hf = \Delta E$ required to excite a proton from the lower to the higher spin state. For a proton in a 1.0 T field the photon energy required is $1.76 \cdot 10^{-7}$ eV corresponding to 42.6 MHz. Thus an radio frequency field (RF) can be applied in order to excite protons to the higher spin state.

An RF field perpendicular to B will also cause the precession of μ_{\perp} around B to be in phase with the RF period. More and more protons getting in phase with the RF will generate a precessing magnetization orthogonal to B , which in turn gives rise to an alternating electromagnetic field causing an RF signal in a pickup coil. By using RF pulses it is thus possible to change the direction of the total magnetization M so it is orthogonal to the external magnetic field B . As the system then gets higher energy it is called excitation. If this was not done, there would be no signal to detect. In this case the total magnetization would not precess, as it is the strength and duration of the RF pulse that determines the orientation of the net magnetization. Typically 90 degrees is desired, which gives maximum signal strength.

Protons precess with a frequency f that depends on the total strength of the external field B . By having a gradient field $G(r)$ added to the constant field B_0 the total field strength will vary with position and particles get different Larmor frequencies [9] depending on their position. The Larmor frequency can be described by the following equation:

$$f = \gamma (B_0 + G(r)) \quad (2.4)$$

where $\gamma = \gamma/2\pi$, γ being the gyromagnetic ratio. For a linear gradient field $G = g \cdot r$ the slope g is the gradient dG/dr , r being position.

The magnetization $M(\mathbf{r}, t)$ of the material can be described with equation 2.5 when the system includes diffusion [10]. The magnetization is then a function over both time and position.

$$\dot{M}(\mathbf{r}, t) = (D\nabla^2 - i\gamma g \cdot r)M(\mathbf{r}, t) \quad (2.5)$$

where D is the diffusion constant, ∇ is the standard del operator and i is the imaginary unit. Solving this differential equation gives the magnetization as a function of both time and position. This under the assumption there are no relaxation processes present [11].

2.3.2 The NMR Signal

If the medium is without boundaries, i.e. free diffusion, the detected signal could approximately be described by [12]

$$S(b) = S_0 e^{-bD} \quad (2.6)$$

where b contains the experimental parameters:

$$b = \gamma^2 g^2 \delta^2 \left(\Delta - \frac{\delta}{3} \right) \quad (2.7)$$

δ represents the duration time of a gradient field pulse and Δ the time between pulses. g is the gradient of the gradient magnetic field. This result is based on e.g. the Pulsed Gradient Spin Echo sequence (PGSE) illustrated in figure 2.1.

The primary NMR signal detected in a coil is an alternating current induced in the coil by the time-varying magnetization field from the studied material. It is given by

$$I(t) = A(t) \cdot \cos(2\pi f \cdot t) \quad (2.8)$$

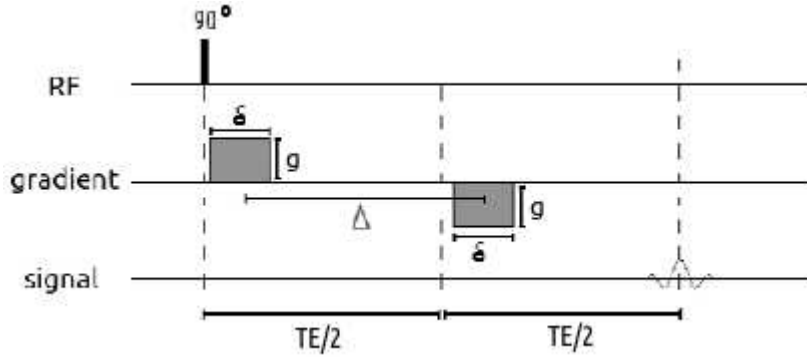


Figure 2.1: A PGSE sequence following an RF pulse. The second gradient pulse causes the particles to rephase and generate a signal maximum after TE.

where f is the frequency. The signal amplitude $A(t)$ gradually decreases with time as the magnetization of the material fades away after excitation (see below). The amplitude then returns to maximum after echo time (TE), see figure 2.1. The signal behavior is similar but reversed before and after TE. In the present study signal decay after TE is utilized. The detected signal is usually Fourier transformed in order to obtain the signal's frequency spectrum [13, 14].

The detected signal can be compared to the signal $S(b)$ given by equation 2.6. The frequency having maximum amplitude in the Fourier spectrum is used as a measure of the detected signal. Its amplitude value (often denoted E) [5] is used as a measure of the signal strength. By plotting the signal E versus the parameter b in logarithmic scale (cf. equation 2.7), the diffusion constant D can be obtained. The parameter b can easily be varied by changing the gradient g of the magnetic field.

In the case of solid matter and a linear gradient field, frequencies of the particles depend on their position. Particles will dephase after excitation and the total signal will decrease over time. If a second gradient with negative polarity is applied, the particles will again rephase. After the same time interval as between the different gradients ($TE/2$ in figure 2.1) all particles will again have the same phase (but not the same frequency) and the signal is back to 100 % (echo signal). After the echo particles will again dephase.

If the studied material is a liquid instead of a solid, the echo signal will not return to 100 %. This is because the molecules will diffuse from one

location p_1 to another p_2 between the gradient field pulses, causing rephasing to be incomplete. A longer time Δ (or stronger diffusion) will give a gradually smaller echo signal until it disappears in the signal noise. It is not only diffusion that affects the echo signal, but also the slope of the gradient field has an influence. It is the difference between the frequency $f(p_1)$ for a particle at p_1 and $f(p_2)$ when it is at p_2 that determines the rephasing efficiency, and thus also what the size of the echo signal will be.

An example is shown in figure 2.2 where $T_i (i = 1, \dots, 5)$ represents five different moments in time separated by equal intervals. The ten particles in a row are particles in a solid material and the single particle is the one that is diffusing in the material. A linear gradient field is applied precisely after T_1 and another one with opposite polarity precisely after T_3 . The particles dephase from T_1 to T_3 and rephase back between T_3 and T_5 . But this will not be the case for the particle that diffuses. Consequently, there will be one less particle pointing exactly in the opposite direction causing slightly smaller magnetization.

2.3.3 Sinus Gradient Field

Instead of having a gradient field which varies linearly in space, a gradient field with a sinusoidal variation is also investigated. Such a field shape was proposed by Grebenkov in 2007 [3] because it offers a considerably simpler mathematical solution. Possibly a sinusoidal field shape will enhance sensitivity for small structures in the studied material. This is an assumption that is investigated in this thesis work.

The sinus gradient field varies in space but it is constant in time. Different spatial wavelengths (λ) of the same order of magnitude as the size of the small structures in the material will be investigated. The NMR signal is assumed to be modulated when $\lambda = 2L$. Figure 2.3 shows the magnetic field including the sinus gradient field in space.

A sinus shaped gradient field component having spatial wavelength λ can be written as

$$G(x) = G_{max} \sin(2\pi x/\lambda) \quad (2.9)$$

The gradient of the field will in this case be

$$\frac{dG}{dx} = G_{max} \frac{2\pi}{\lambda} \cos(2\pi x/\lambda) \quad (2.10)$$

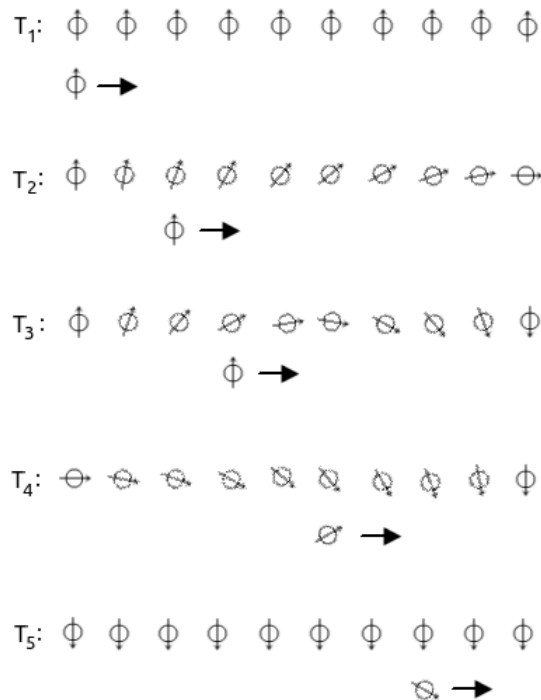


Figure 2.2: Spin orientation as a function of position at five different times. A diffusing particle will however be out of sync.

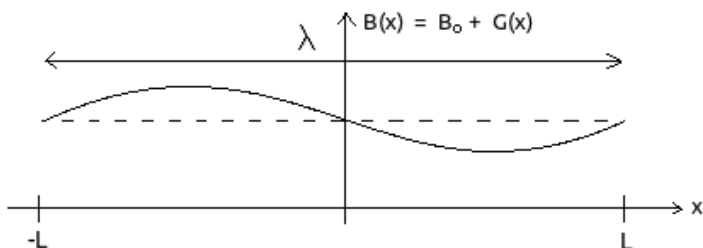


Figure 2.3: Illustrates a sinus shaped gradient field component $G(x)$ on top of the constant magnetic field B_0 (dashed line). Diffusion boundaries are at $\pm L$.

which will replace the constant gradient g in expression 2.7 for the parameter b .

Chapter 3

Method of Investigation

Equation 2.5 is difficult to solve analytically (involves a non-Hermitian operator). The problem becomes even more complicated when boundaries are present in the diffusion material. Numerical methods have to be used which is done with computer simulations. The present work has been to construct a computer simulation code to study the influence of material structures that give boundaries to the diffusing mechanism in the material.

3.1 The Monte Carlo Code

The computer simulation technique used in this work is based on computer-generated random numbers, a technique often referred to as Monte Carlo technique. The random numbers generated by standard computer algorithms are uniformly distributed between 0 and 1. A good computer random number generator should have a very long cycle (examples of 10^{38} numbers exists) and every limited sequence should be uniform over the interval $[0,1]$.

The method of simulating a complex many-particle phenomenon like diffusion is to follow the trajectory of the diffusing particles as it moves through the material. Each collision point is randomly chosen according to previous collision, mean range and isotropy. In the present simulation a set of particles were followed parallel in time.

3.1.1 Code Structure

To get an overview of how the program operates a flow chart is illustrated in figure 3.1. Firstly, all constants where defined: diffusion constant (D), the magnitude of the external magnetic field (B), number of particles (N),

number of how many runs that were made with different gradients, each giving a specific echo decay (ED), number of time steps between the gradient pulses (Δ), number of time steps the gradients were applied (δ) and the gyromagnetic ratio (γ). Secondly, the program looped over the different gradient cases, and each specific gradient (g) was defined inside the loop. The simulation of a gradient case then started by choosing random starting positions for a set of diffusing particles, i.e. initial r values. Once r values had been assigned the Larmor frequencies f were calculated for every particle. The particle drift was simulated over time by following them step by step. For every time step in loop $*_1$ to $*_4$ a new direction (θ) and range (dr) of the particles were calculated if the particle did diffuse. Also the Larmor frequencies of the particles (f), their phases (ϕ) and the current induced in the coil (I) were calculated. In $*_1$ and $*_3$ the gradient is applied and in $*_2$ and $*_4$ there is only diffusion. For every gradient case (ED) the maximum value of the Fourier transform (E) of the signal is saved and b (see equation 2.7) is calculated and saved. After all gradient cases were simulated the E signals were plotted versus b .

3.1.2 Particle Sources

To start with, all particles in the simulation were emitted from one and the same point. Later when the code was further developed the particle start position was spread randomly and uniformly inside of an interval. As the interval was different from $[0,1]$ the random numbers R needed to be converted. This can be achieved by multiplying R with the interval range $2L$, and then subtracting with half the interval L witch gives:

$$x = (2R-1) \cdot L \quad (3.1)$$

For the two dimensional case the source region was a quadratic area. The individual particle's start position (x, y) should then be chosen at random inside this area, and should be uniformly distributed. This is achieved by calculating both x and y according to the above expression.

3.1.3 Particle Direction

In the one dimensional case the particles only have two directions to travel, negative or positive. The probability of each is 0.5 and the direction can be simulated by determining if a random number is below or above 0.5. Depending on that decision, they travel in negative or positive direction. For two dimensional diffusion the unit directional vector should point with equal

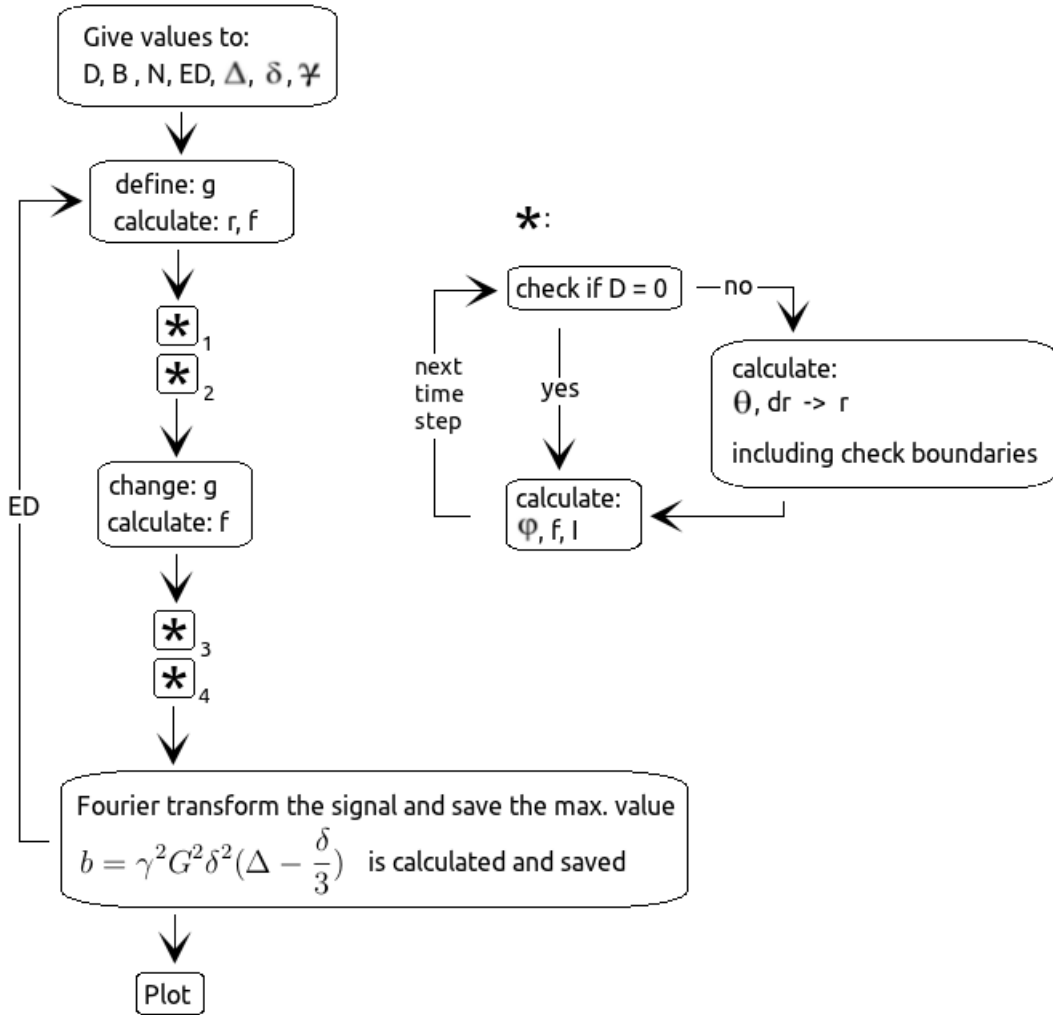


Figure 3.1: Flow chart illustrating the overall program structure.

probability in any directions in the plane. This is achieved by calculating the angle ϕ using

$$\phi = R \cdot 2\pi. \tag{3.2}$$

The vector components are then calculated as $x = \cos(\phi)$ and $y = \sin(\phi)$.

3.2 The Different Investigations

In the first part of the work only diffusion was investigated, first in one dimension, then in two dimensions. In the second part of the work (sec. 3.2.2 to 3.2.5) particle spin and NMR signal were simulated as well. In both parts diffusion was free or restricted by material boundaries.

3.2.1 Diffusion

As a start, a simulation program was written for particles diffusing freely without boundaries in only one dimension. Particles were all started at the same point taken to be the origin of a coordinate system. The diffusion process was simulated by considering time steps corresponding to the time interval between two consecutive particle collisions. After each collision the particle drift direction and the path length for the next step was chosen randomly (cf. sec. 3.1.2). Direction was thrown isotropically. The particle range should be picked from an exponentially decreasing distribution but can be considered approximately uniform if the time step is short. This gives a small effect which makes diffusion slightly worse than in reality. The distribution of diffusing particles was plotted versus time. 200 particles were traced for 100 steps. To get a measure of how fast the particles diffuse from their start positions the Mean Square Displacement (MSD) was calculated. MSD is a common way to describe the extension of the particle distribution and is normally used in problems including random walk. The definition of MSD in one dimension (x) gives the following result [6]:

$$MSD \equiv \langle (x(t) - x_0)^2 \rangle = \dots = 2Dt \quad (3.3)$$

where D is the diffusion constant. To get a good estimate of the MSD at least 5000 particles had to be simulated for 200 time steps. More particles were used successively to obtain better statistics and to get an estimate of the accuracy in the MSD value.

As a second investigation the program was complemented with a routine that generates a random start position inside an interval. The end points of the interval $[-20, 20]$ were acting as walls reflecting the diffusing particles back into the interval. If a particle traveled outside the interval, its drift direction was simply flipped at the boundaries, so it continued to travel the remainder of its range inside the interval in opposite direction (figure 3.2). As in the first investigation the particles' distribution in space as developing over time was plotted for 5000 particles versus 200 time steps. MSD relative

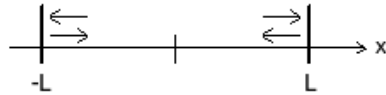


Figure 3.2: In the one dimensional case particles are reflected at boundaries.

to the particle starting position was also computed and plotted for 5000 particle versus 400 time steps.

As a third investigation drift in two dimensions was simulated. The particle source was taken to be a single constant point, and particles were also started in random positions uniformly distributed inside a two dimensional box. The boundary conditions were set to be periodic. When a particle diffuse across a boundary, it is translated to the opposite side boundary and will continue inside the interval area with the same direction, as shown in figure 3.3. Simulating this is equivalent to study a limited region inside an infinite material. In both cases 200 particles were generated and traced for at least 100 steps. The resulting spatial distribution was plotted. To obtain an accurate histogram 100 000 particle were needed used for 400 time units. For both two-dimensional cases the MSD was calculated for 2000 particles after 200 steps.

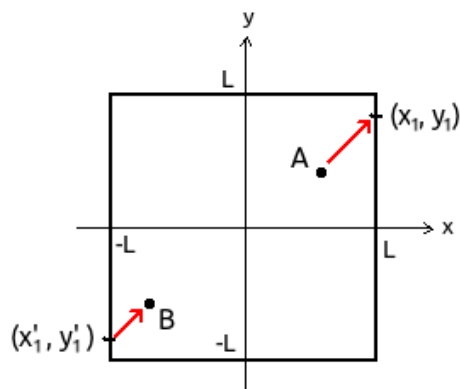


Figure 3.3: In the two dimensional case particles are transposed to the oppsite boundary so that $x'_1 = -x_1$ and $y'_1 = -y_1$.

3.2.2 Magnetization

Once the code had been demonstrated to simulate diffusion correctly, the magnetization of the material and the NMR signal strength were simulated. A magnetic field with a constant gradient, i.e. linear dependence, was added to the program code simulating one dimensional diffusing with random starting positions. After each step when tracing the diffusing particle, its x position was used for r in equation 2.4 to compute the field strength at that position. Subsequently, the particle's Larmor frequency could be calculated. Throughout all simulations the value of the gyromagnetic constant was set to $42.59\text{MHz}/T$, which is the number valid for hydrogen, being most commonly used in clinics. Finally the NMR signal is given by the sum over all particles as described in section 2.3.2.

When programming complex problems it is necessary to reduce them to a number of steps which are easily tested. Therefore in the present case a solid material was first simulated without diffusion. A gradient magnetic field was applied at the first time step, and at a later time step a second gradient was applied with negative slope instead. As described in sec. 2.3.2 this should give back a full echo signal [5]. A simulation was made with 10 000 particles. If particles diffuse, the signal will be smaller as described in the same section. Larger diffusion constant gives smaller echo signal. To demonstrate this fact the program was run with five different values of the diffusion constant: 0, 0.010, 0.020, 0.025 and 0.030 all with 70 000 particles.

3.2.3 NMR Signal

Another effect than diffusion which decreases the signal strength is a stronger field gradient. Thus, the next step was to compare the signal for different gradient strengths. This was done by taking the Fourier transform of the signal, using the maximum amplitude and plot it versus b , see equation 2.7. In the case of a linear gradient and free diffusion the function should be a line in logarithmic scale with the slope $-D$ [5]. Two runs were made for free diffusion in two dimensions, each with the same set of different linear gradients but with different diffusion constant values: 0.002 and 0.006. For the run with low diffusion constant 20 000 particles were used, whereas 150 000 had to be used for the run with high diffusion constant. The signal would otherwise be too small to reach above the noise level. In the PGSE sequence the δ -time interval was set to one time unit, and Δ -time interval was set to 500 time units. These values were used throughout all investigations.

3.2.4 Material Structure

The same experiment was simulated again but now with two boundary planes, which is a simple simulation of a structured material. Periodic boundary conditions are still applied in the perpendicular direction to these planes. Because the diffusion is no longer free the detected signal will not show a simple exponential decay. Instead, the signal will show a number of broad peaks on a negative slope in logarithmic scale. This is described mathematically by Barzykin [10] and simulated by Linse and Söderman [4]. Two runs were made with the same diffusion constant 0.018, but different separation between planes being 0.10 and 0.12 length units, respectively. In this case those two values were chosen to reduce run time for 100 000 particles, which were needed to obtain good statistics.

The first step to study a more complicated structure than two planes is to have a passage with two different widths instead of one. It should give a superposition of the two individual signals. Each signal had been calculated earlier. The two widths that the program was coded for were 0.10 and 0.12 length units so it could be compared with the earlier results. Here were 400 000 particles used.

3.2.5 Sinusoidal Field

The last investigation studied the effect of a magnetic field having a dependence according to a sinus function. In this case the wavelength of the sinus function was varied instead of the slope of the gradient field. The hypothesis is that the NMR signal will depend on the match between spatial wavelength and the separation between boundaries, i.e. the structure size of the material. These simulations were made both for free diffusion and diffusion restricted by two planes. Theoretically the problem has been solved by Grebenkov [3]. The echo decay function should start as a plateau and then fall off with a steep slope for the case of free diffusion. When the particles diffuse between two planes, the function should show a tail with a periodic structure including a number of small peaks. Depending on the diffusion constant value the plateau will be long or hardly distinguishable.

Two runs were made for the case of free diffusion, having the same field varying gradient but different diffusion constants. One with a diffusion constant value of 0.005 for 70 000 particles and one run with a diffusion constant value of 0.0015 for 5000 particles. In the case of diffusion between planes, three runs were made for different parameter combinations. In the first two

runs the distance between the planes were 0.22 length units and 0.10 length units, respectively, while the set of wavelengths were kept constant. In the third run separation between planes was kept at 0.10 length units while the set of wavelengths now was changed. Run time limited the number of particles to 1 000 000.

Chapter 4

Results

The different investigations carried out in this work can be referred to studies of the diffusion mechanism on one hand (sec. 4.1), and the simulations of the NMR signal on the other hand (sec. 4.2). The second part includes several different cases of boundary conditions and gradient field shapes.

4.1 Diffusion

Figure 4.1 shows the tracing of particles over time as they diffuse freely in one dimension starting at the origin. The growing of the width of the distribution over time is evident. How fast the distribution width grows is easier to see by plotting MSD versus time, which is presented in figure 4.2. It is a clear linear dependence indicating that the particles diffuse at a constant rate, which is consistent with diffusion theory.

Next, the particle start position was chosen randomly and uniformly within an interval between boundary planes. The particle tracing over time is plotted in figure 4.3. As expected particles appear to be occupying the entire interval uniformly. To see the actual diffusion in this case MSD has to be plotted, which is shown in figure 4.4. Since the particle diffusion is limited by boundaries, the MSD will not increase linearly but approach a constant value as seen in the figure.

Figure 4.5 shows particle tracing in two dimensions with a starting position at the origin. The figure clearly shows a random-walk pattern as expected. The distribution of particle positions after some time is presented in figure 4.6. The shape is following a two dimensional Gaussian function as it should. This is because the particle diffusion is free and linear, which also is seen from

a linearly increasing MSD as figure 4.7 shows.

The result from the two dimensional case with random start position is presented by the histogram in figure 4.8. The histogram shows particle position after a certain diffusion time. It can be seen that the distribution is still generally uniform. The calculated MSD can be seen in figure 4.9. The MSD does not approach a constant value as in the one dimensional case, since the boundaries in this two dimensional case are periodic. Because periodic boundaries are equivalent to a free diffusion case, MSD will increase linearly.

4.2 NMR

The simulated detected signal for a solid material and linearly varying gradient field in a PGSE sequence is presented in figure 4.10a. It can be seen how the signal initially decays and how the echo signal is built up. As previously described particles dephase because of their different frequencies and then rephase because of the second gradient field pulse. As can be seen from the graph the second gradient was applied after 300 time units since the echo signal appears after 600 time units. Figure 4.10b to 4.10f illustrate the detected signal when the particles diffuse with different values of the diffusion constant, see table 4.1. Figure 4.10b corresponds to the smallest value and figure 4.10f to the largest value. It is clearly seen that the echo signal decreases with larger diffusion constant value.

Figure 4.11 presents how the echo decay signal E (cf. sec. 2.3.2) changes for free diffusion, when the linear gradient field strength g is varied as a function of b , see equation 2.7. The red coloured distribution corresponds to larger diffusion constant, whereas the blue distribution corresponds to smaller diffusion constant, as evident from the different slope. Figure 4.12 and 4.13 presents the echo decay signal in the same way but now having diffusion between two boundary planes. Both distributions in the two figures have the same diffusion constant value but different range between boundary planes, figure 4.12 being the short range case. The anticipated broad peak structures are clearly visible. Their detailed shapes depend on both the diffusion constant and the range between the planes.

Figure 4.14 presents the echo decay signal E as a function of b for free diffusion and with a sinus shaped gradient field. In this case g in equation 2.7

is a function of a spatial wavelength of the sinus shaped field. The dependence should show a plateau followed by a sharp decrease. In this scale it is difficult to see any plateau, but it could indicate that the diffusion constant actually is rather large. Figure 4.15 presents the echo decay signal E versus b for diffusion between boundary planes. The beginning of the distribution is dominated by free diffusion. Further out on the tail the limiting effect of the two planes start to influence as the slope changes. On the tail of the distribution there could be small peaks in a periodic structure. Poor statistics makes, however, such structure difficult to see. In figure 4.16 the boundary planes were placed closer together, see table 4.2 for parameter values. The effect from the boundary planes appears to start earlier in this distribution than in the one in figure 4.15. In figure 4.17 the set of spatial wavelength values is changed. The data points of the distribution seem to be bunched differently.

In Figure 4.18 the echo decay signal E is presented for diffusing particles between two pairs of boundary planes. The gradient field was in this case once again linear. It is here possible to see that the result seems to be a superposition of the result in figure 4.12 and 4.13. The first broad peak appears in figure 4.18 because the individual peaks from figure 4.12 and 4.13 coincide. Further out on the tail the two structures get more out of phase and cancel each other. With improved statistics a small structure on the tail would occur. Evidently the structure of the material will influence the signal behavior.

Table 4.1: Different values chosen for the diffusion constant when simulating traces in figure 4.10.

| Figure | Diffusion constant, D | | | |
|--------|-----------------------|-------|-------|-------|
| 4.10 | 0.010 | 0.020 | 0.025 | 0.030 |

Table 4.2: Listed are parameter settings for all simulations shown in figures 4.11 – 4.18. $\delta = 1$ and $\Delta = 500$ are used in all cases.

| Figure | Distance | Diffusion const., D | Grad. type | Grad. interval |
|--------|---------------|---------------------|------------|----------------|
| 4.11 | - | 0.006 and 0.002 | linear | [0.0033,0.033] |
| 4.12 | 0.10 | 0.018 | linear | [0.0033,0.033] |
| 4.13 | 0.12 | 0.018 | linear | [0.0033,0.033] |
| 4.14 | - | 0.005 and 0.0015 | sinus | [0.12, 0.54] |
| 4.15 | 0.22 | 0.0015 | sinus | [0.12, 0.54] |
| 4.16 | 0.10 | 0.002 | sinus | [0.12, 0.54] |
| 4.17 | 0.10 | 0.002 | sinus | [0.06, 0.25] |
| 4.18 | 0.10 and 0.12 | 0.018 | linear | [0.0033,0.033] |

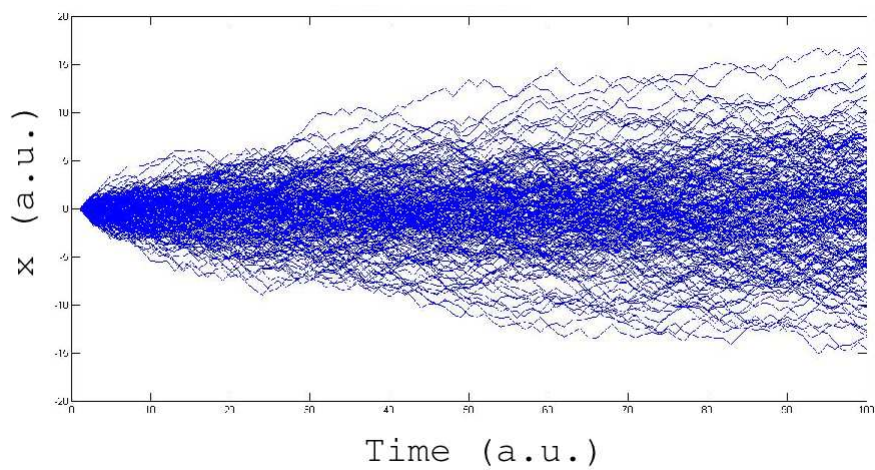


Figure 4.1: The diffusion tracing for free diffusion particles in one dimension over time. The particle source point is at the origin.

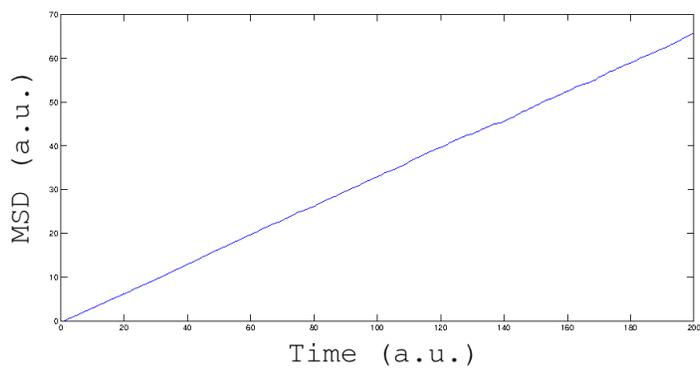


Figure 4.2: MSD for free diffusion particles in one dimension over time.

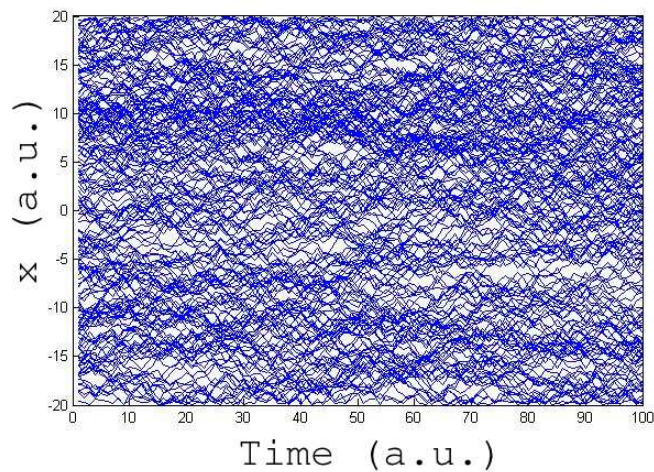


Figure 4.3: The diffusion tracing for particles with free diffusion in one dimension over time. The particle start position is uniformly placed at random in a closed interval.

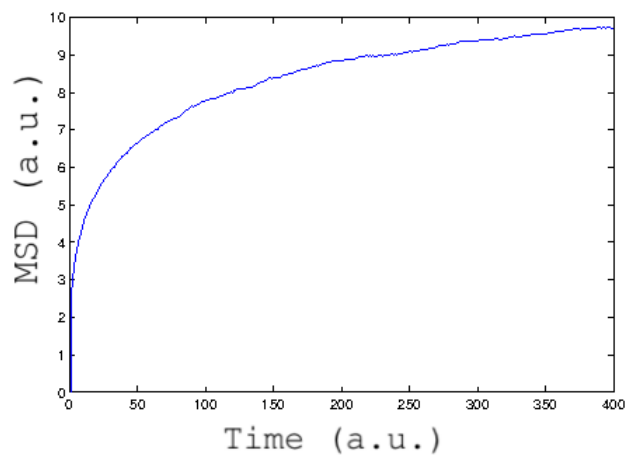


Figure 4.4: MSD for the particles diffusing inside a closed interval in one dimension over time.

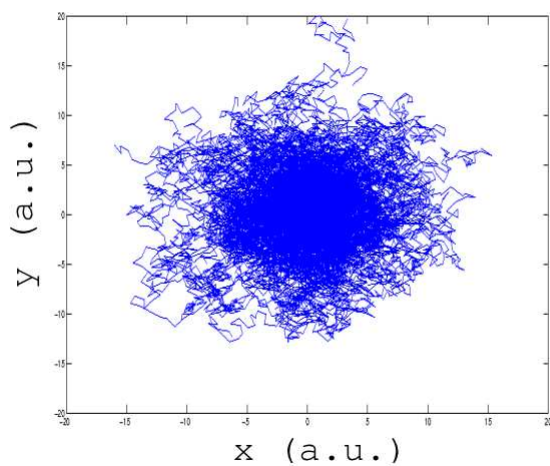


Figure 4.5: The diffusion paths for particles diffusing freely in a plane. They all start at the origin.

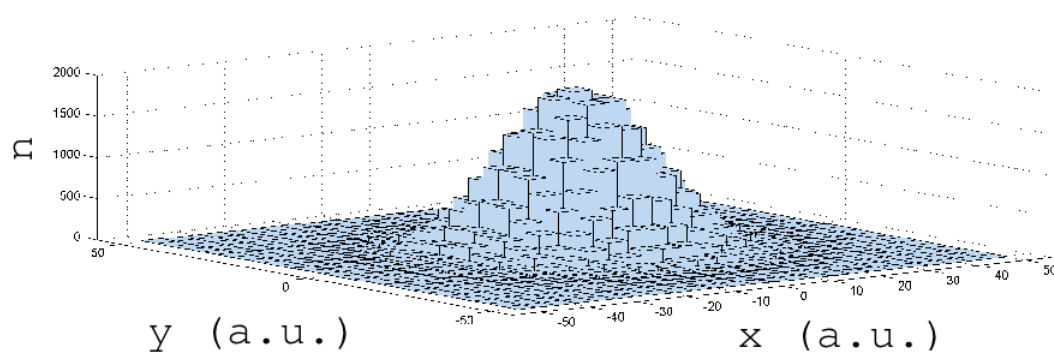


Figure 4.6: Freely diffusing particles in two dimensions. Shown is the distribution after certain diffusion time starting from the origin.

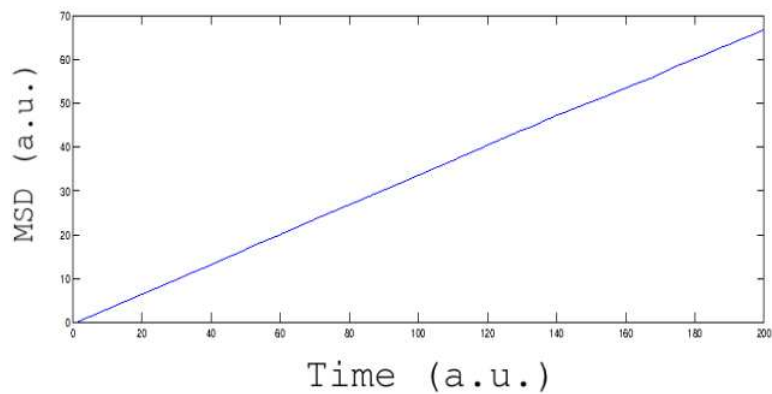


Figure 4.7: MSD for particles diffusing freely in the plane and starting at the origin.

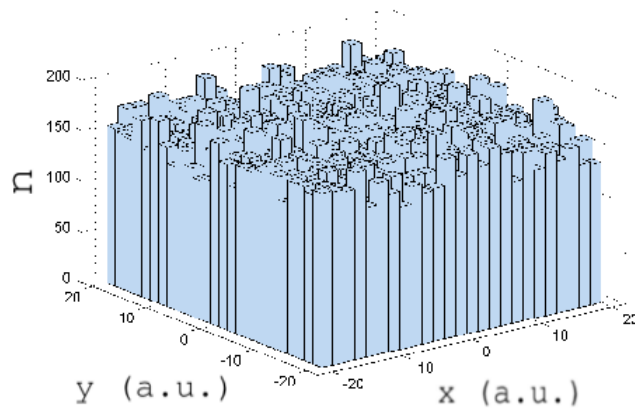


Figure 4.8: Particle distribution (n) after certain diffusion time. Particles' start positions are chosen uniformly within the square area and diffusion is free with periodic boundaries.

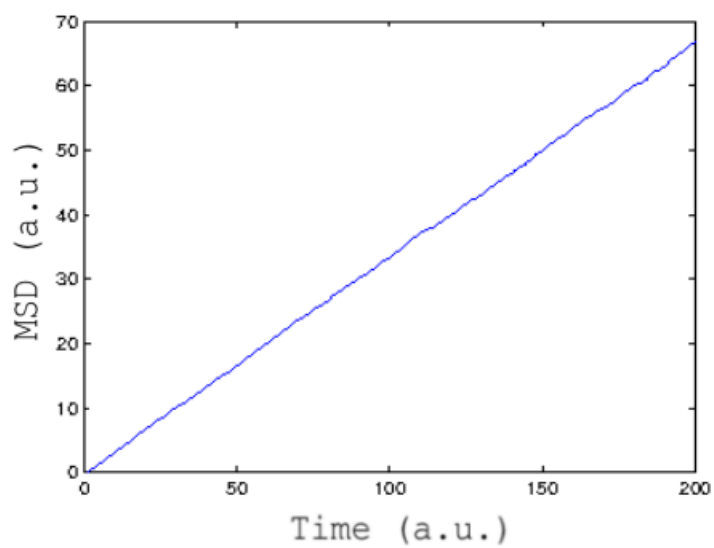


Figure 4.9: MSD for particles diffusing inside a two dimensional box with periodic boundaries. Conditions are same as figure 4.8.

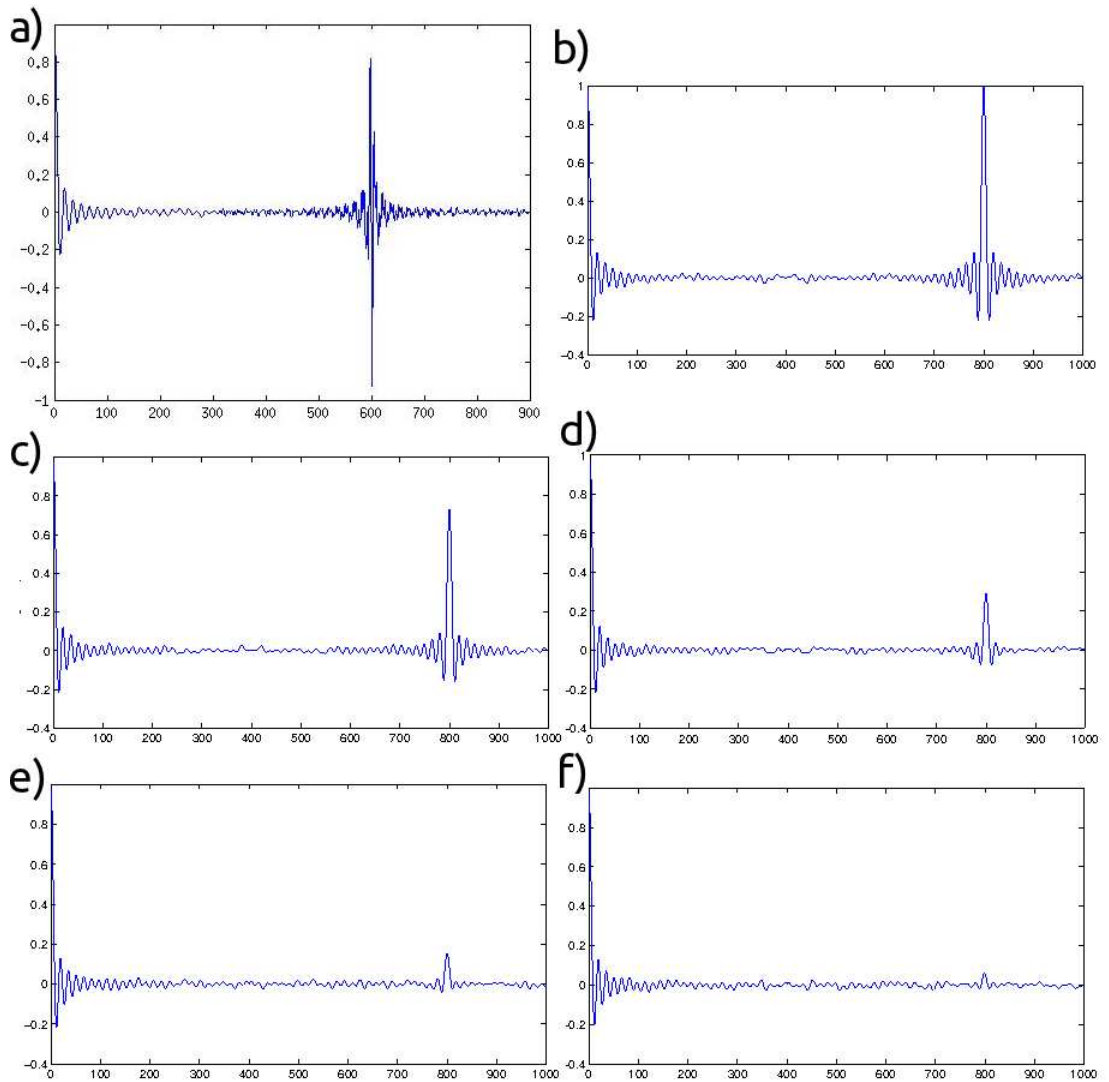


Figure 4.10: Shown is the coil signal for six different cases, a) solid material without diffusion, b)-f) materials with increasing amount of diffusion. Plotted is current (a.u.) vs. time (a.u.). Notice how the echo signal gradually vanishes with increasing diffusion.

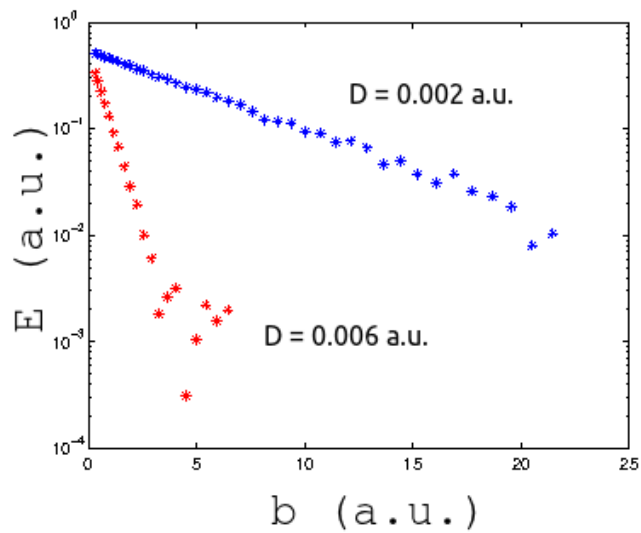


Figure 4.11: Plotted is the echo decay signal E vs. the parameter b (see sec. 2.3.2 for definition) for two different cases as indicated of freely diffusing particles.

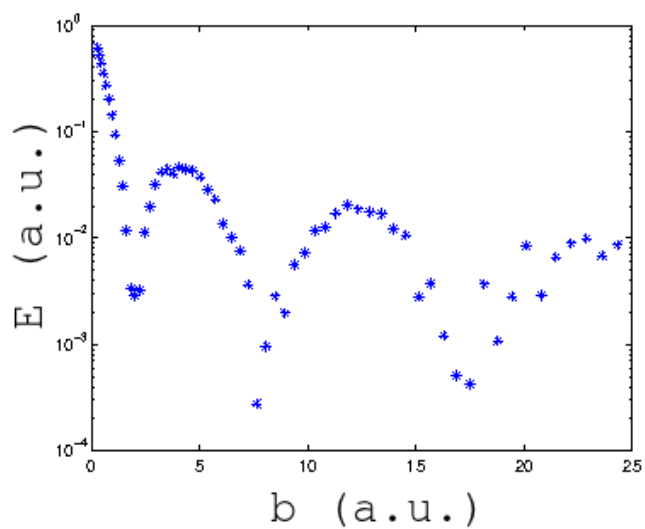


Figure 4.12: Same as figure 4.11 (blue case) but restricted diffusion between boundaries.

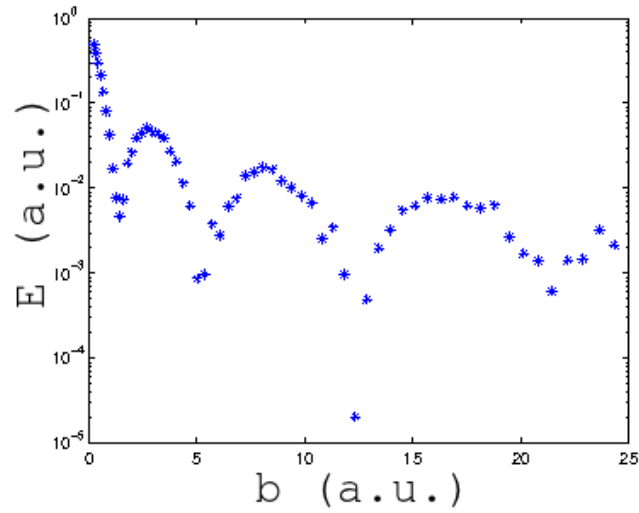


Figure 4.13: Same as figure 4.12 but with 20% larger distance between boundaries.

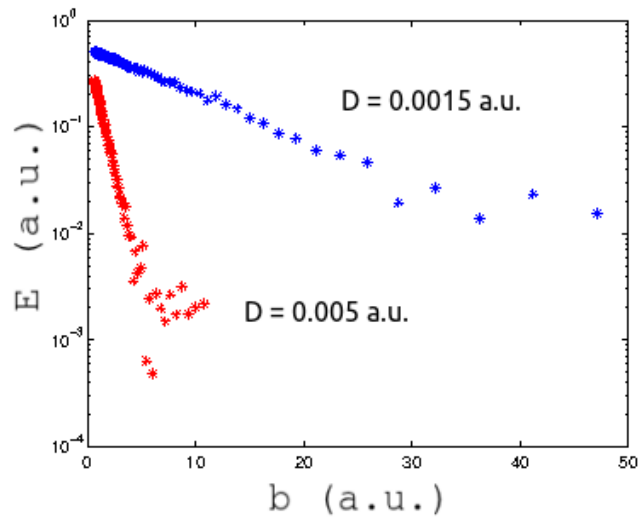


Figure 4.14: Same as figure 4.11 but for a sinusoidal gradient magnetic field. The parameter b depends on the spatial wavelength λ of the sinusoidal field.

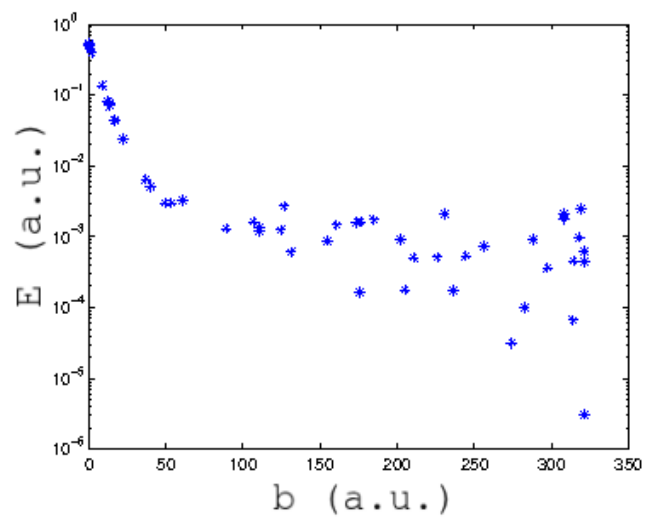


Figure 4.15: Same as figure 4.14 but diffusion restricted between boundaries. λ varies between approximately $4L$ (left end) and L (right end), $2L$ being distance between boundaries.

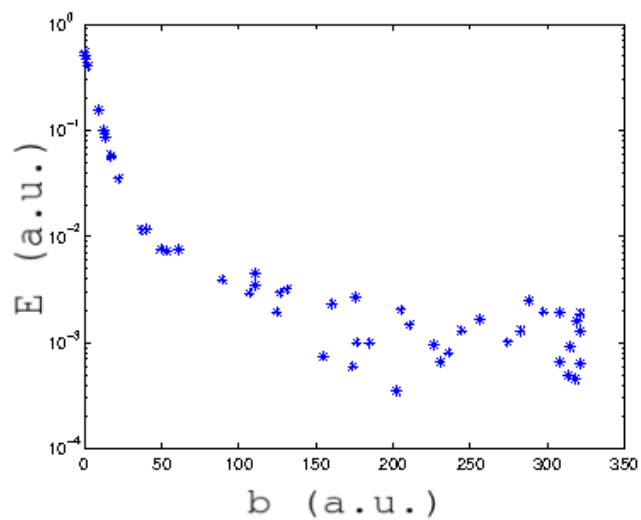


Figure 4.16: Same as figure 4.15 but the distance between boundaries reduced by 50%. λ not changed.

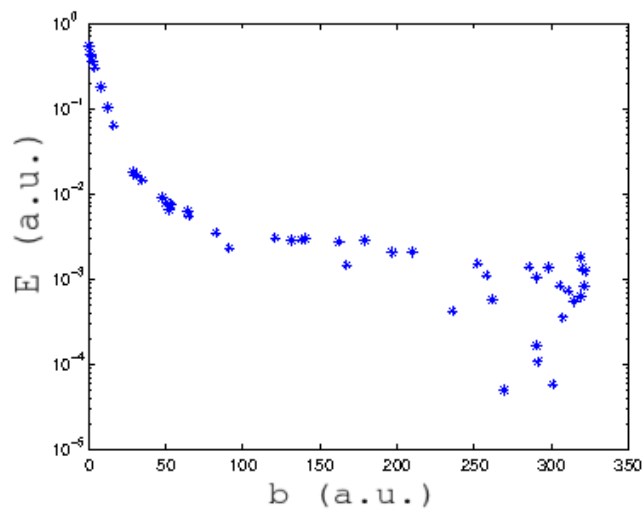


Figure 4.17: Same as figure 4.16 but λ adjusted to shorted boundaries distance.

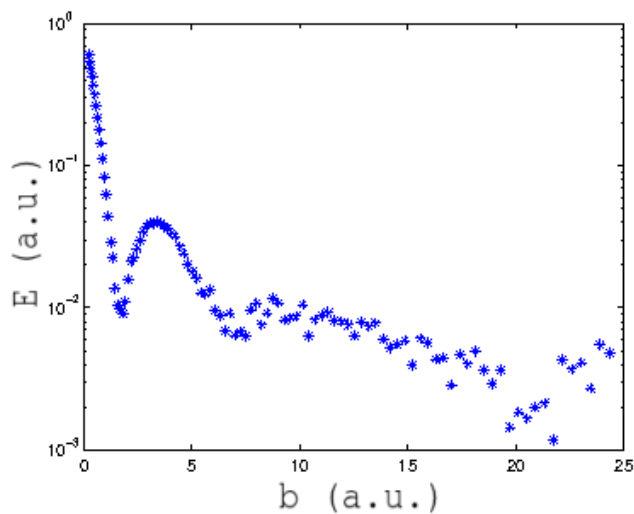


Figure 4.18: Same as figures 4.12 and 4.13. The shorter distance between boundaries (4.12) applies to half the diffusion plane, while the larger distance (4.13) applies to the other half.

Chapter 5

Discussion and Conclusions

The simulation code was developed step by step to make debugging efficient. The first task was to simulate the diffusion process. For these purposes the MSD was calculated, since the particle behavior in figures 4.1, 4.3, 4.5, 4.6 and 4.8 is difficult to interpret only from the figures themselves. Simulating diffusion is a standard problem and the results were in agreement with theory.

Once diffusion was correctly simulated, the second task was to simulate the NMR mechanism. Figure 4.10 demonstrates that the signal has been correctly computed from the theory. The fact that the echo signal decreases with larger diffusion constant is a strong indication that the simulation is correct. Figure 4.10b through 4.10f are all generated with the same number of particles so that they easily can be compared. The number of particles in the simulation run was chosen as low as possible to optimize run time while still obtaining a clear signal.

The signal E in figure 4.11 should start at 1.0 since it is normalized. Instead it appears to start below 1.0 at the origin. This is probably due to that the diffusion started before the signal was detected. In the coding this means that the first signal was calculated after the first step and not before. The same effect can be seen in all figures 4.11 – 4.18. This coding feature was discovered late in the process and therefore not corrected. It is in principle insignificant since it only corresponds to a time shift. When studying diffusion and material structure one typically rescales E values to obtain $E(0) = 1$. In figure 4.12 the distribution drops faster than in figure 4.13. Since the distance between the boundary planes is larger in figure 4.13, the diffusion fraction which does not hit the planes should be larger and the dependence should be more like free diffusion. Thus, the broad peaks are smaller and the slope is not that steep.

Next, the NMR signal behavior for a sinus shaped gradient field will be discussed. In figure 4.14 one would expect a short plateau before the immediate linear fall-off. In case of a large diffusion constant (red distribution) the steep slope could make it difficult to resolve a short plateau. In case of a small diffusion constant (blue distribution), on the other hand, the weak slope and a longer plateau could make the onset of the fall-off hard to see at the end of the distribution. The trend of the distributions in figures 4.15 – 4.17 clearly shows a general shape starting with a rapid fall-off and followed by a less steep tail with oscillations indicating possible peaks. This is a clear indication that the Fourier transform is correct. The data points in figure 4.15 – 4.17 appear to scatter irregularly. One interpretation is that it has to do with the choice of wavelength interval in relation to the distance between boundary planes. If the distance between the boundary planes is too large, diffusion will tend to wash out the spin correlation, and consequently the signal will be severely influenced by statistical fluctuation. In the two first figures 4.15 and 4.16 the data behaves similarly in the b direction, whereas it behaves differently in figure 4.17 where the wavelength interval was altered to fit the distance between the boundary planes. At data point number 13 the wavelength exactly matches the distance between the boundary planes. So it is around this point one might expect the behaviour to change. After this point there will be more than one period of the sinus function between the boundary planes.

No statistical uncertainties have been accurately calculated in this project. It is a complicated statistical problem that would have required too much time. It should have been interesting though, to know the statistical quality of the result.

An important result of this work is that the shape of the distribution of E versus b clearly depends on the actual distance between the confining boundary planes. This is evident from the case with a linear gradient field. By comparing figures 4.12 and 4.13 it is possible to see that the superposition should give a shape like the one in figure 4.18. This implies that the influence of material structure on diffusion of particles in fact does effect the NMR signal.

A suggested way to continue these investigations would firstly be to make an analysis of statistical accuracy. For the case with a linear gradient field, next step would be to find a way to calculate the small distances in a material's structure from its distribution of E versus b . For a sinus shaped gradient field it would be interesting to vary the tail structure by different parameter

settings. Then, the subsequent study would be to simulate more complex materials and investigate if the signal is interpretable.

Acknowledgement

First and most of all I am deeply grateful to my supervisors Matias Nordin for all support and patience, and for giving me the opportunity to do such an interesting master thesis work in a most exciting field of science research.

I am also very grateful to my assistant supervisor Maja Sohlin for proof reading this report and giving many valuable comments.

I want to thank my friends Christian, Eidel and Adam for helping setting up my computer environment and giving me useful guidance with the programming.

Finally, I wish to thank my fellow student and dear friend Sabina for helpful comments and discussions.

Bibliography

- [1] E. M. Purcell et al. Resonance absorption by nuclear magnetic moments in a solid. *Journal of Physical Review*, 69:37–38, 1946.
- [2] H. Y. Carr and E. M. Purcell. Effects of diffusion on free precession in nuclear magnetic resonance experiments. *Journal of Physical Review*, 94:630–638, 1954.
- [3] D. Grebenkov. Nuclear magnetic resonance restricted diffusion between parallel planes in a cosine magnetic field: An exactly solvable model. *Journal of Chemical Physics*, 126, 2007.
- [4] P. Linse and O. Söderman. The validity of the short-gradient-pulse approximation in NMR studies of restricted diffusion. simulations of molecules diffusing between planes, in cylinders and spheres. *Journal of Magnetic Resonance, Series A*, 116(1):77–86, 1995.
- [5] W. S. Price. Pulsed-field gradient nuclear magnetic resonance as a tool for studying translational diffusion: Part 1. Basic theory. *Concepts in Magnetic Resonance*, 9(5):299–336, 1997.
- [6] H-U. Bengtsson. Om halvklassisk fysik. *Studentlitteratur*, 2000.
- [7] A. Einstein. On the movement of small particles suspended in stationary liquids required by the molecular-kinetic theory of heat. *Annalen der Physik*, 17:549–560, 1905.
- [8] J. J. Sakurai. *Modern Quantum Mechanics (Revised Edition)*. Addison Wesley, 1 edition, September 1993.
- [9] B. H. Bransden and C. J. Joachain. *Quantum Mechanics*. Prentice-Hall, 2 edition, 2000.
- [10] A V Barzykin. Theory of spin echo in restricted geometries under a step-wise gradient pulse sequence. *Journal of Magnetic Resonance*, 139(2):342–353, 1999.

- [11] William S Price. *NMR Studies of Translational Motion*. Cambridge University Press, 2009.
- [12] M. J. Graves D. W. McRobbie, E. A Moore and M. R. Prince. *MRI From Picture to Proton*. Cambridge University Press, second edition, 2007.
- [13] G. B. Arfken and H-J. Weber. *Mathematical Methods for Physicists*. Academic Press, sixth edition, 2005.
- [14] James Keeler. *Understanding NMR Spectroscopy*. John Wiley & Sons Ltd, second edition, 2010.